Received: 13 September 2019 | Revised: 12 November 2019 | Accepted: 12 November 2019

DOI: 10.1002/rcm.8660

SPECIAL ISSUE RESEARCH ARTICLE

WILEY Rapid Communications in Mass Spectrometry

Limitations of ion mobility spectrometry-mass spectrometry for the relative quantification of architectural isomeric polymers: A case study

Romain Liénard[1,2] | Quentin Duez[1] | Scott M. Grayson[3] | Pascal Gerbaux[1] | Olivier Coulembier[2] | Julien De Winter[1]

[1] Interdisciplinary Center for Mass Spectrometry, Organic Synthesis and Mass Spectrometry Laboratory, University of Mons—UMONS, Mons, Belgium

[2] Center of Innovation and Research in Materials and Polymers, Laboratory of Polymeric and Composite Materials, University of Mons—UMONS, Belgium

[3] Department of Chemistry, Tulane University, New Orleans, Los Angeles, USA

Correspondence
J. De Winter, Interdisciplinary Center for Mass Spectrometry, Organic Synthesis and Mass Spectrometry Laboratory, University of Mons – UMONS, 23 Place du Parc, 7000 Mons, Belgium.
Email: julien.dewinter@umons.ac.be

Funding information
Research and Innovation Staff Exchange (RISE), Grant/Award Number: BIODEST H2020-MSCA-RISE-2017-778092

Rationale

Since their discovery, cyclic polymers have attracted great interest because of their unique properties. Today, the preparation of these macrocyclic structures still remains a challenge for polymer chemists, and most of the preparation pathways lead to an inescapable contamination by linear by-products. As the properties of the polymers are closely related to their structure, it is of prime importance to be able to assess the architectural purity of a sample.

Methods: In this work, the suitability of ion mobility spectrometry-mass spectrometry (IMS-MS) for the quantification of two isomers was investigated. A cyclic poly(L-lactide) was prepared through photodimerization of its linear homologue. Since IMS-MS can be used to differentiate cyclic polymer ions from their linear analogues because of their more compact three-dimensional conformation, the present work envisaged the use of IMS-MS for the quantification of residual linear polymers within the cyclic polymer sample.

Results: Using the standard addition method to plot calibration curves, the fraction of linear contaminants in the sample was determined. By doing so, unrealistically high values of contamination were measured.

Conclusions: These results were explained by an ionization efficiency issue. This work underlines some intrinsic limitations when using IMS-MS in the context of the relative quantification of isomers having different ionization efficiencies. Nevertheless, the linear-to-cyclic ratio can be roughly estimated by this method.

1 | INTRODUCTION

The development of modern materials science allows the preparation of numerous complex polymer architectures such as star-shaped polymers,[1] dendrimers,[2] or cyclic polymers.[3] Since their discovery, cyclic polymers have attracted great interest because of their unique properties directly related to the absence of chain-ends.[4,5] To this day, the quantitative preparation of the macrocyclic structures is still considered a great challenge in polymer science. The synthetic pathways of macrocyclic polymers can be divided into two main categories: the ring-expansion strategy and the ring-closure strategy. Both have been extensively reviewed during the past few years.[6-9] Most of the developed methods inescapably lead to the cyclic macromolecules being contaminated with their linear counterparts. As the biological and physical properties of the polymers are closely related to their structure, it is of prime importance to be able to assess the architectural purity of a sample, or at least to quantify the extent of contamination.[10]

In this context, most traditional polymer characterization techniques have proved to be unsuitable for the detection of trace

amounts of these contaminants. In fact, the quantification by proton nuclear magnetic resonance (^{1}H NMR) and Fourier-transform infrared (FT-IR) can be based only on the signals that are specific to the chain-ends of the linear contaminants. However, because of a lack of sensitivity of ^{1}H NMR and FT-IR, the corresponding signals are often overwhelmed by those of the polymer backbone, leading to an inaccurate (under)estimation of the impurities. In addition, spectroscopic techniques only afford an averaged overview of the sample that could be problematic if intermolecular coupling is present. Size-exclusion chromatography (SEC) is another commonly used technique for polymer characterization. Because their two chain-ends are connected to each other, cyclic polymers have less conformational freedom than their linear analogues, resulting in a lower hydrodynamic volume for a given degree of polymerization (DP).[11] However, the low resolving power of SEC most of the time prevents the detection of small quantities of contaminants (< 5%).[12]

Finally, mass spectrometry (MS) has become more popular for polymer characterization, as confirmed by the significantly increasing number of published papers combining polymer synthesis and MS. Indeed, due to the development of soft ionization sources, such as matrix-assisted laser desorption/ionization (MALDI) and electrospray ionization (ESI), MS in combination with NMR and SEC has become almost unavoidable for polymer characterization.

Single-stage MS cannot discriminate two isomer ions because they possess the same mass-to-charge ratio (*m/z*). However, most of the time, collision-induced dissociation mass spectrometry (CID-MS) can be useful for that purpose. By applying the survival yield (SY) method developed by Memboeuf et al for isobaric species[13] and isomeric ions, Josse et al successfully detected and succeeded in quantifying as little as 2% of linear contaminants in a *cyclo*-poly(L-lactide) (*c*-PLLA) sample prepared through a ring-closure strategy by the copper-catalyzed azide-alkyne cycloaddition (CuAAC) "click" reaction.[14] The SY method takes advantage of the significant difference among the energy thresholds (E_{50}) at which the isomeric ions corresponding to the cyclic and the linear species dissociate. Nevertheless, this method cannot be applied to isomer ions that inconveniently fragment at similar energy thresholds, and another technique is then required in that case.

Ion mobility spectrometry-mass spectrometry (IMS-MS) is an emerging technique for the characterization of polymers.[15-17] IMS-MS measures the drift time, in the gas phase, of ions accelerated under the application of an electric field through a mobility cell filled with a buffer gas. Large ions characterized by high collision cross sections (CCSs) will experience more collisions with the buffer gas than more compact ions (with lower CCSs) and thus will be more delayed during their journey through the mobility cell, resulting in a higher drift time than the low CCS ions. The drift time of ions can thus be related to their three-dimensional (3D) structure in the first approximation. Hoskins et al reported the use of IMS-MS to differentiate cyclic and linear isomers of poly(ε-caprolactone) (PCL).[17]

In the present work, we investigate whether IMS experiments can be envisaged to quantify the relative proportion of isomeric macromolecules within a synthetic mixture. To achieve this objective, we prepare an original *c*-PLLA through photodimerization of a linear tailor-made anthracene end-capped PLLA analogue. We then expose the the corresponding ions to IMS separation on a *T-Wave*-based instrument and monitor the IMS separation all along the polymer distribution. Synthetic mixtures of linear/cyclic polymers are prepared for the relative quantification of the isomeric polymers based on the relative abundances of the IMS-separated ions.

2 | EXPERIMENTAL

2.1 | Materials

All reagents were purchased from Merck (Darmstadt, Germany) and used without further purification unless otherwise noted. L-Lactide (L-LA) (≥ 99%) was purchased from Galactic (Escanaffles, Belgium), recrystallized from dried toluene three times, and stored in a glove box under a dry nitrogen atmosphere (O_2 < 5 ppm; H_2O < 1 ppm) prior to use. CH_2Cl_2 and 1,4-butanediol were dried over CaH_2 for 48 h at room temperature, distilled under reduced pressure, and stored in a glove box under a dry nitrogen atmosphere. *N*,*N*,*N*′,*N*′′,*N*′′-Pentamethyldiethylenetriamine (PMDETA) was dried over $MgSO_4$ and stored in a glove box. Acetonitrile (ACN) (≥ 99.5%) used was of analytical grade. 1,8-Diazabicyclo[5.4.0]undec-7-ene (DBU) was purchased from Fluka (Buchs, Switzerland), dried over BaO, distilled, and stored in a glove box. Copper(I) bromide was purified by washing it with acetic acid. 11-Azido-1-undecanol, 4-pentynoic anhydride, and 9-anthracenecarbonyl chloride were synthesized as reported in the literature.[18-20]

2.2 | Instrumentation

SEC was performed in tetrahydrofuran at 35°C using a liquid chromatograph equipped with a PL-DG802 degasser (Polymer Laboratories, Church Stretton, UK), an isocratic HPLC pump LC 1120 (flow rate = 1 mL min^{-1}), a Marathon autosampler (loop volume = 200 µL, solution concentration = 1 mg mL^{-1}), a PL-DRI refractive index detector, and three columns: a PL gel 10 µm guard column and two PL gel Mixed-B 10 µm columns (linear columns for separation of MW_{PS} ranging from 500 to 10^6 Da). Polystyrene standards were used for calibration.

IMS-MS experiments were performed using a Synapt G2-*Si* mass spectrometer (Waters, Wilmslow, UK) equipped with an electrospray ionization (ESI) source. All the solutions were directly infused into the ESI source using a Pump 11 Elite syringe pump (Harvard, Holliston, MA, USA) with a typical flow rate of 5 µL min^{-1}, a capillary voltage of 3.1 kV, a source temperature of 100°C, and a desolvation temperature of 200°C. The ion mobility parameters were set as follows: wave height, 40 V; wave velocity, 800 m s^{-1}; trap gas flow rate (Ar), 10 mL min^{-1}; helium cell gas flow rate, 180 mL min^{-1}; IMS gas flow rate (N_2), 70 mL min^{-1}; traps bias, 40 V. IMS-MS data were analyzed using Waters Masslynx software. Arrival time distributions (ATDs) were recorded by selecting the most abundant isotope for

each polymer ion. Deconvolution and fitting of the ATD were performed using Origin 2016 (OriginLab, Northampton, MA, USA).

2.3 | Preparation of the samples

A stock solution of linear polymer **1** was prepared by dissolving 5 mg of polymer **1** in 10 mL ACN and diluting that solution 10-fold followed by another 25-fold to obtain 10 mL of a 2 ng mL^{-1} solution. To that solution, 30 µL of a 2 mg mL^{-1} LiI solution was added.

A stock solution of cyclic polymer **2** was prepared by sampling 1 mL directly from the 20 mg L^{-1} cyclization reaction solution after completion of the cyclization and diluting it 10-fold to obtain a 2 ng mL^{-1} solution. To that solution, 30 µL of a 2 mg mL^{-1} LiI solution was added.

The different samples were prepared by mixing the corresponding ratios of the stock solutions of polymers **1** and **2** to keep a total polymer concentration of 2 ng mL^{-1}.

2.4 | Synthetic procedures

2.4.1 | Preparation of 11-azidoundecyl-anthracene-9-carboxylate ester

A glass vial was charged with 500 mg 9-anthracenecarbonyl chloride (2 mmol), 5 mL CH_2Cl_2, 486 mg 11-azido-1-undecanol (2.2 mmol), and 290 µL triethylamine (2 mmol). After 8 h under stirring at room temperature, 15 mL CH_2Cl_2 was added, and the organic phase was extracted with a saturated $NaHSO_4$ aqueous solution, dried over $MgSO_4$, filtered, and evaporated using a rotary evaporator. 11-Azidoundecyl-anthracene-9-carboxylate ester was recovered as a yellow paste (yield: 70%).

^{1}H NMR (500 MHz, $CDCl_3$, δ, ppm): 1.29 (m, 12, -O $(CH_2)_3(CH_2)_6(CH_2)_2N_3$), 1.49 (m, 2, -O $(CH_2)_2CH_2(CH_2)_8N_3$), 1.59 (m, 2, -O $(CH_2)_9CH_2CH_2N_3$), 1.88 (m, 2, -$OCH_2CH_2(CH_2)_9N_3$), 3.24 (t, 2, -O $(CH_2)_{10}CH_2N_3$), 4.62 (t, 2, -$OCH_2(CH_2)_{10}N_3$), 7.51 (m, 4, 4ArH), 8.04 (t, 4, 4ArH), 8.53 (s, 1, ArH).

2.4.2 | Preparation of α,ω-dihydroxy-poly(L-lactide)

In a glove box under nitrogen atmosphere (O_2 < 5 ppm; H_2O < 1 ppm), a first glass vial was charged with 1.0 g L-LA (7 mmol) and 9.0 g CH_2Cl_2. A second glass vial was charged with 1.0 g CH_2Cl_2, 30 µL 1,4-butanediol (1,4-BD) (0.35 mmol; $n_{L\text{-}LA}/n_{1,4\text{-}BD}$ = 20), and 105 µL DBU (0.7 mmol; $n_{DBU}/n_{1,4\text{-}BD}$ = 2). The content of the second vial was transferred to the first one. After 1 min, the polymerization was quenched by the addition of 93 mg benzoic acid (0.77 mmol). The polymer was recovered by precipitation from CH_2Cl_2 into cold methanol (MeOH). $M_n^{SEC,\ app}$ = 6100 g mol^{-1}; $Đ^{SEC}$ = 1.13; M_n^{MALDI} = 3200 g mol^{-1}; $Đ^{MALDI}$ = 1.06.

2.4.3 | Preparation of α,ω-dialkyne-poly(L-lactide)

A glass vial was charged with 300 mg α,ω-dihydroxy-PLA (M_n^{MALDI} = 3000 g mol^{-1}) (1.0 × 10^{-4} mol), 10 mL CH_2Cl_2, 53 µL 4-pentynoic anhydride (3.0 × 10^{-4} mol), and 24 mg 4-(dimethylamino) pyridine (2.0 × 10^{-4} mol). After 24 h, 10 mL CH_2Cl_2 was added, and the organic phase was extracted twice with a saturated $NaHCO_3$ aqueous solution, twice with a saturated $NaHSO_4$ aqueous solution, dried over $MgSO_4$, filtered, and concentrated using a rotary evaporator. The polymer was recovered by precipitation from CH_2Cl_2 into cold MeOH. $M_n^{SEC,\ app}$ = 6200 g mol^{-1}; $Đ^{SEC}$ = 1.13; M_n^{MALDI} = 3600 g mol^{-1}; $Đ^{MALDI}$ = 1.05.

2.4.4 | Preparation of α,ω-dianthryl-poly(L-lactide) 1

In a glove box under nitrogen atmosphere (O_2 < 5 ppm; H_2O < 1 ppm), a glass vial was charged with 150 mg α,ω-dialkyne-PLA (M_n^{MALDI} = 3200 g mol^{-1}) (4.7 × 10^{-5} mol), 41 mg 11-azidoundecyl-anthracene-9-carboxylate ester (1.0 × 10^{-4} mol), 1 mL CH_2Cl_2, 1.3 mg copper (I) bromide (1.0 × 10^{-5} mol), and 2 µL PMDETA (1.0 × 10^{-5} mol). After 8 hours under stirring, 15 mL CH_2Cl_2 was added, and the organic phase was extracted with a saturated $NaHSO_4$ aqueous solution, dried over $MgSO_4$, filtered, and concentrated using a rotary evaporator. The polymer was recovered by precipitation from CH_2Cl_2 into cold MeOH. $M_n^{SEC,\ app}$ = 7200 g mol^{-1}; $Đ^{SEC}$ = 1.13; M_n^{MALDI} = 4400 g mol^{-1}; $Đ^{MALDI}$ = 1.03.

2.4.5 | Preparation of *cyclo*-poly(L-lactide)

Ten milligrams of α,ω-dianthryl-PLA (M_n^{MALDI} = 4200 g mol^{-1}) (2.4 × 10^{-6} mol) was dissolved in 500 mL of ACN. The polymer solution was irradiated for 12 h at room temperature using two compact low-pressure fluorescent lamps (Arimed B6, Cosmedico GmbH, Stuttgart, Germany) emitting at 320 nm (±30 nm) in a custom-built photoreactor. The solvent was then evaporated using a rotary evaporator, and the polymer was recovered without any further purification. $M_n^{SEC,\ app}$ = 5900 g mol^{-1}; $Đ^{SEC}$ = 1.15; M_n^{MALDI} = 4350 g mol^{-1}; $Đ^{MALDI}$ = 1.03.

3 | RESULTS AND DISCUSSION

cyclo-Poly(L-lactide) **2** (*c*-PLLA; $M_n^{SEC,\ app}$ = 5900 g mol^{-1}; $Đ^{SEC}$ = 1.15) is prepared by ring-closure of a telechelic α,ω-dianthryl-PLLA linear precursor **1** (*l*-PLLA; $M_n^{SEC,app}$ = 7200 g mol^{-1}; $Đ^{SEC}$ = 1.13) (Figure 1) through a photo-induced [4 + 4] cycloaddition using a homemade photoreactor as described by Josse et al in the experimental part for previous cyclization experiments.[21] Tezuka and coworkers have already used this strategy for the preparation of cyclic poly(ethylene oxide) (PEO) and cyclic poly(tetrahydrofuran) (PTHF) and showed that having an electron-withdrawing group such as a carbonyl on the anthryl groups is required to reach an apparent quantitative cyclization.[22] The full synthetic pathway to **1** is described in

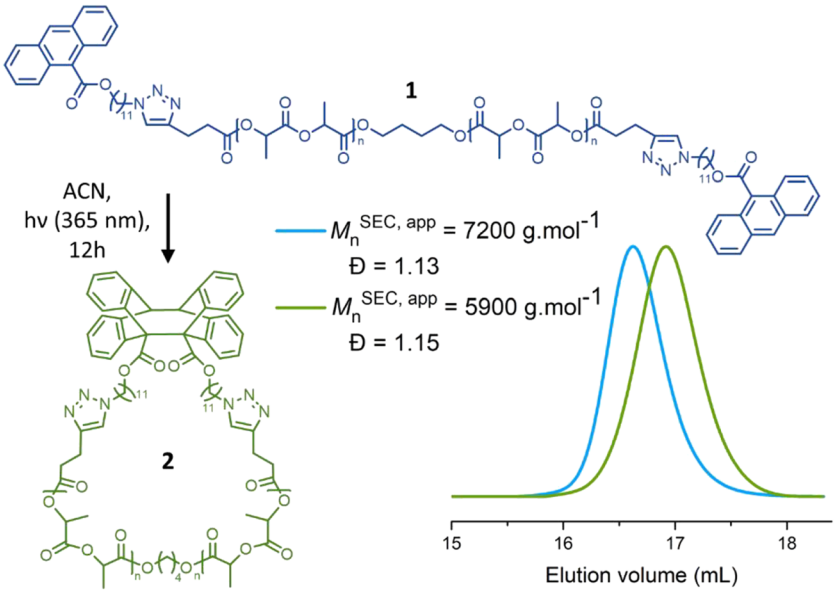

FIGURE 1 Cyclization of *linear*-poly(L-lactide) (*l*-PLLA) to *cyclo*-poly(L-lactide) (*c*-PLLA): experimental conditions and corresponding SEC traces [Color figure can be viewed at wileyonlinelibrary.com]

Scheme SI1 (supporting information). Precursor and intermediates have been characterized by ^{1}H NMR and MALDI-TOF (Figures SI1–S4, supporting information). Finally, both **1** and **2** have been fully characterized by MALDI-TOF, ^{1}H NMR, and SEC to confirm their structure and the efficiency of the light-induced cyclization (Figure 1; and Figures S4–S6, supporting information). Nevertheless, the presence of residual linear precursors within the cyclic sample is not detected by SEC and hardly observed using ^{1}H NMR. In addition, it is expected that the relative proportion of the residual linear polymers will depend on the DP, because the cyclization efficiency is dependent on the chain length. Indeed, as explained by the Jacobson-Stockmayer theory,[23] the probability of the two chain-ends meeting within the capture volume and then reacting decreases as the chain lengthens. Consequently, the weight distribution of macrocyclic constituents at equilibrium is often shown to be a monotonically decreasing function of the molecular size.[24]

Ion mobility experiments on ESI-generated polymer ions are often more informative than those on MALDI-generated ions because ESI produces multiply charged ions whose gaseous structures are affected by the coulombic repulsion between the cationizing particles, that is, Na^+ cations in the positive ion mode. The ESI mass spectra of the pure *l*-PLLA and the (contaminated) *c*-PLLA samples are presented in Figure 2; both spectra feature the dominant production of 3+ ions, say [*l*-PLLA +3Na]$^{3+}$ and [*c*-PLLA +3Na]$^{3+}$ ions. The major differences between these two spectra are the quasi-absence of 4+ ions and the higher abundance of the 2+ charged ions for the cyclic sample. This difference can be related to the limited conformational freedom that the cyclic macromolecules have compared with their linear counterparts, making them less amenable to accommodating numerous cations.

As a first quantitative approach, the SY technique developed by Josse et al has been tested on the 3+ ions of both the *l*-PLLA and

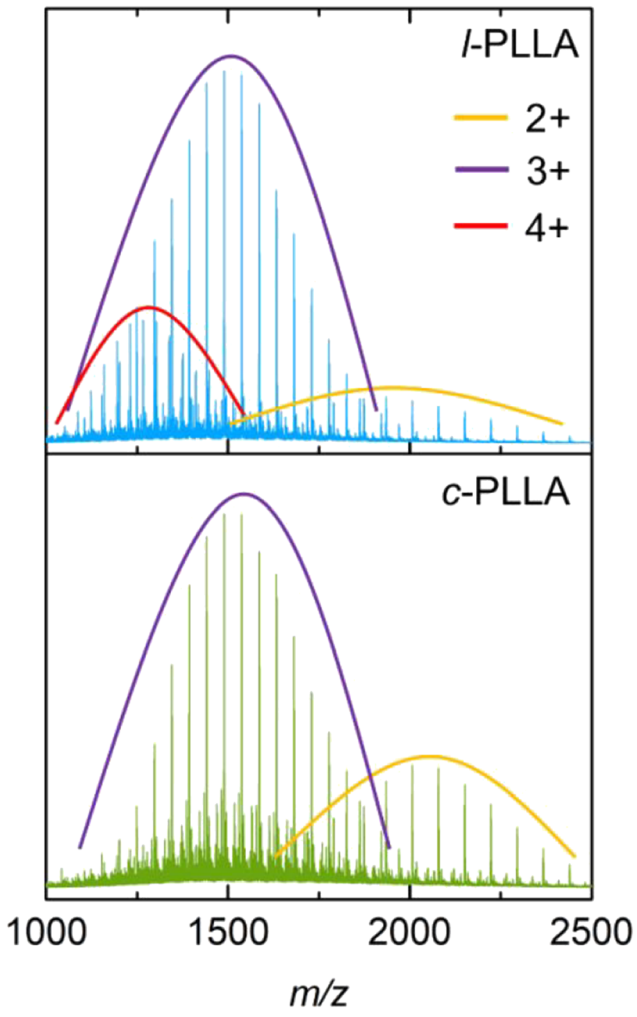

FIGURE 2 Electrospray mass spectra of *l*-PLLA (top) and *c*-PLLA (bottom) samples [Color figure can be viewed at wileyonlinelibrary.com]

the *c*-PLLA samples. Unfortunately, this method is not efficient in quantifying the residual linear polymers within the cyclic samples. Indeed, as mentioned before, the prerequisite for using the SY method for isomer quantification is that the fragmentation thresholds for the linear and cyclic ions need to be significantly different. However, as presented in Figure 3, when recording the corresponding SY curves, we observe that the 3+ polymer ions, say $[l\text{-PLLA}_{20} + 3Na]^{3+}$ **1** and $[c\text{-PLLA}_{20} + 3Na]^{3+}$ **2**, fragment at roughly the same energy threshold. The origin of this similarity is discussed later in the paper.

The *l*-PLLA and *c*-PLLA 3+ ions are then exposed to ion mobility separation with special attention paid to the evolution of the ATDs all along the ion series; that is, increasing DP. As presented in Figure 4, we observe that the 3+ linear and cyclic isomers are readily separated due to IMS-MS,[17] but only for ions having a DP below 24–25. This is readily explained by the known behavior of multiply charged polymer ions that adopt a spherical shape only when the multiple charges present in the gaseous ions are fully screened from each other by the polymer chain atoms.[25,26]

It is now well documented that such stabilization is a stepwise process experimentally detected by monitoring the evolution of the ATD of polymer ions for increasing polymer chain length (increasing DP). Usually, multiply charged polymer ions with a low DP will adopt an extended structure to minimize the coulombic repulsion between the charges. But as the DP increases, the additional monomer units will screen this electrostatic effect and permit the charges to get closer to each other, up to a point where a large enough macromolecular ion will adopt a completely globular conformation.[25,27,28] As already reported for 3+ linear PLA ions, different structures, that is, from extended to folded ions, coexist during this process (Figure 4). It is also confirmed that no interconversion between the different 3D structures is possible.[26] However, for cyclic polymer ions, which are constrained by their topology, one main 3D structure is observed. Therefore, whereas at a low DP, cyclic and linear polymer ions can be readily separated using IMS-MS, it is no longer possible to differentiate these isomeric ions after their complete folding at larger DP because they will adopt fully folded/spherical conformations and thus will present similar drift times (Figure 4).

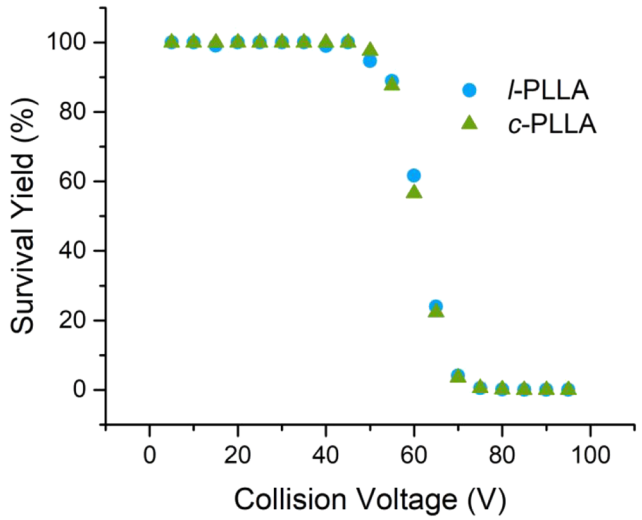

FIGURE 3 Survival yield curves of *m/z* 1345 ions for $[l\text{-PLLA}_{20} + 3Na]^{3+}$ **1** and $[c\text{-PLLA}_{20} + 3Na]^{3+}$ **2** [Color figure can be viewed at wileyonlinelibrary.com]

A closer analysis of the IMS data presented in Figure 4 reveals that the ATDs of the $[l\text{-PLLA} + 3Na]^{3+}$ ions are complex and span a wide range of arrival times. As a typical example, the ATD of the $[l\text{-PLLA}_{20} + 3Na]^{3+}$ ions extends from 8 to 11 ms (Figure 5A), due to the presence of coexisting 3D structures (i.e., partially extended and folded) and also due to the existence of isomeric $l\text{-PLLA}_{20}$ molecules. Indeed, the PLLA polymer under investigation (see Figure 1) is constituted by two PLLA blocks – likely to be of different lengths – separated by the butanedioxy residue. Interestingly, upon cyclization, this broad isomer distribution is no longer detected by IMS-MS, as depicted in Figure 4. This is associated with the loss of conformational freedom upon cyclization limiting the differences between the isomers.

Figure 5 shows the MS-CID-IMS-MS spectra for the linear and cyclic isomers at collision voltages (CVs) of 5 V and 45 V, respectively. As observed in Figure 3, the 45 V collision voltage is just before the dissociation threshold of both $[l\text{-PLLA}_{20} + 3Na]^{3+}$ and $[c\text{-PLLA}_{20} + 3Na]^{3+}$ ions (*m/z* 1345). At 5 V and 45 V collision voltages, the ATDs of the *m/z* 1345 linear ions emerging from the trap cell are found to be nearly identical (Figures 5A and 5B). However, this is no longer the case for the cyclic counterparts. First, at 5 V, an intense signal at around 7.5 ms is ascribed to the $[c\text{-PLLA}_{20} + 3Na]^{3+}$ ions. This signal is followed by a trace of lower intensity attributed to $[l\text{-PLLA}_{20} + 3Na]^{3+}$ ions due to their typical ATD signature (Figure 5C). Second, upon ion activation at 45 V, even if no fragmentation is observed (see Figure 3), the ATD profile for the cyclic isomer is significantly modified, demonstrating that activated cyclic ions undergo a ring-opening process, resulting in a quantitative conversion back to their linear form before fragmentation (Figure 5D). This observation explains why the breakdown curves are superimposable for the two isomers, as depicted in Figure 3, rendering the SY quantification procedure inefficient in our case. The [4 + 4] anthracene photodimerization is known to be thermally reversible in solution,[29] and our results reveal that, upon collisional activation, retro-cycloaddition reactions can be promoted. Another example of thermal isomerization induced by collisional activation between ionized photo-isomers has been recently reported and concerns azobenzene-based photoswitches.[30]

Therefore, the linear polymer ions observed at low collision voltage in Figure 5C could originate from (a) partial opening of the cyclic isomer upon collisional activation even at very low collision voltage or (b) a non-quantitative cyclization reaction. To investigate the origin of the observed linear polymer trace, MS-CID-IMS-MS experiments are performed at different collision voltages. Figure 6 reports the evolution of the cyclic polymer trace over the total area of the IMS trace for *m/z* 1345 $[c\text{-PLLA}_{20} + 3Na]^{3+}$ ions. Significant ring-opening can be observed at voltages as low as 10 V.

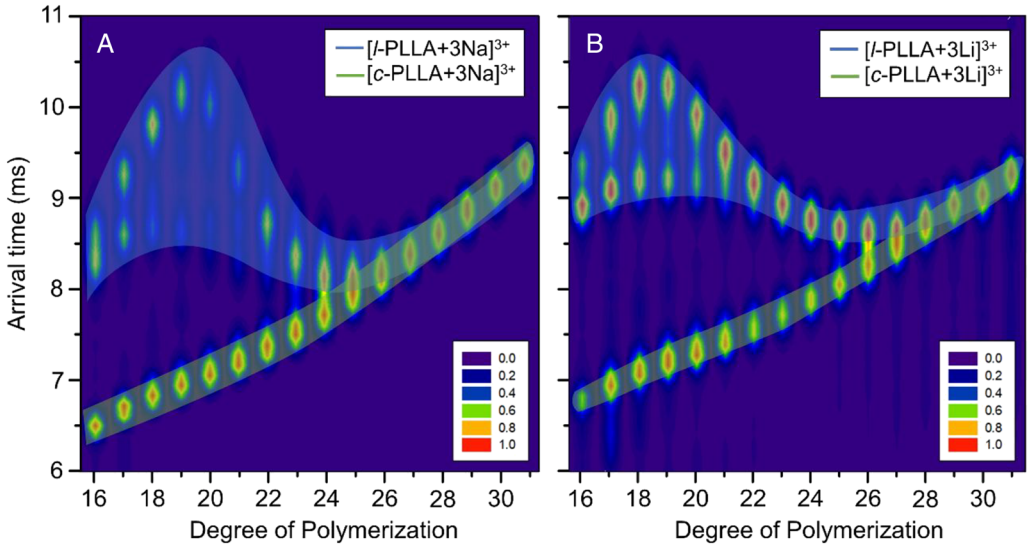

FIGURE 4 Arrival time (t_A) versus degree of polymerization (DP) for A, [*l*-PLLA +3Na]$^{3+}$ and [*c*-PLLA +3Na]$^{3+}$ and B, [*l*-PLLA +3Li]$^{3+}$ and [*c*-PLLA +3Li]$^{3+}$. Both datasets are recorded for a 5:5 (cyclic:linear) mixture [Color figure can be viewed at wileyonlinelibrary.com]

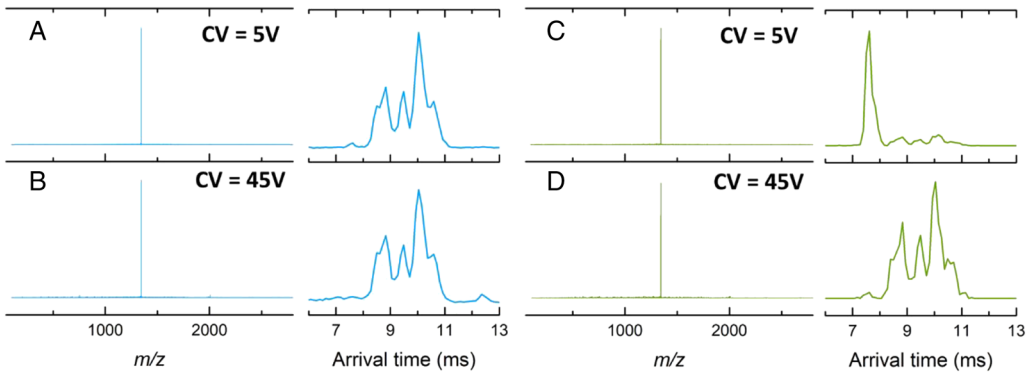

FIGURE 5 MS-CID-IMS-MS experiments on the *m/z* 1345 ions ([*l*-PLLA$_{20}$ + 3Na]$^{3+}$ **1** and [*c*-PLLA$_{20}$ + 3Na]$^{3+}$ **2** in the trap cell at A, C, 5 V and B, D, 45 V): CID spectra and arrival time distributions (ATDs) of the precursor/product ions [Color figure can be viewed at wileyonlinelibrary.com]

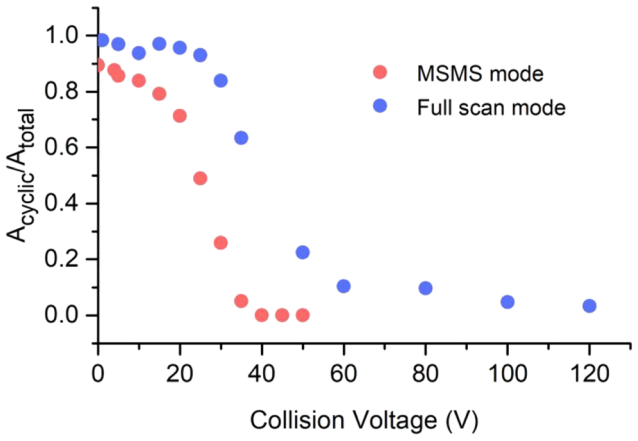

FIGURE 6 Area ratio of the cyclic polymer trace and the total ion mobility spectrometry-mass spectrometry (IMS-MS) trace in MSMS and full-scan modes for *m/z* 1345 [*c*-PLLA$_{20}$ + 3Na]$^{3+}$ ions [Color figure can be viewed at wileyonlinelibrary.com]

Interestingly, when full-scan CID-IMS-MS experiments are performed, the initial intensity of the linear polymer trace is significantly weaker and the energy required to open the *c*-PLLA is substantially higher than that during the MS-CID-IMS-MS experiments. Indeed, as reported in Figure 6, although the proportion of linear isomers increases drastically from 10 V in MS-CID-IMS-MS, at least 30 V is needed to induce a noticeable ring-opening in full-scan mode. No straightforward explanation is available to account for such a difference. A minute comparison of the pressure in the trap cell and all the applied voltages from the ion source to the mobility cell do not reveal any difference between the full-scan and the MSMS modes. One possibility is that, without any mass selection before the IMS separation, the trap cell (where the CID processes occur) is populated with a considerably higher number of ions than in the MSMS mode, affecting in one way or another the activation of ions. Whatever its origin, this observation is verified for any DP, provided that linear/cyclic discrimination is

achieved by IMS-MS, and for both Na^+ and Li^+ as the cationizing agent, as presented in Figure S7 (supporting information). In full-scan IMS mode, as the experimental conditions appear to be softer, the presence of the linear trace can thus be attributed only to the presence of residual linear polymer in the starting material. We can now evaluate IMS as a good alternative to the SY method for the linear/cyclic quantification, keeping in mind that this is applicable only in the presence of multiply charged ions of a relatively low DP because of the folding phenomenon.[26]

In the context of this work, for the considered samples, we focus our investigations on the triply charged polymer ions. As mentioned earlier, differences can be observed using IMS only before the folding of the chain. Globally, transitions between extended and compact structures, the so-called foldings, are observed for ions presenting more than one charge, meaning that the doubly charged ions could also be considered. However, the folding for doubly charged ions is observed at very low DPs (<15) that are not present in the current sample. The $[M + 3Na]^{3+}$ ions could *a priori* appear as good candidates, provided that ions with different DPs present resolved ATDs for the linear and cyclic isomers. As presented in Figures 4 and 5, the ATDs of the $[M + 3Na]^{3+}$ ions appear complex and DP-dependent, rendering the standardization of the procedure problematic. We, therefore, probe Li^+ ions as the cationizing particles, and we observe that the ATDs are significantly simplified, even for the 3+ ions, when the Li^+ ions replace the Na^+ ions (Figure 7). We will soon study molecular dynamics simulations to understand the Li^+/Na^+ differences. But, for the present paper, we only consider the $[M + 3Li]^{3+}$ ions to simplify the quantification procedure based on signal integration. We monitor the evolution of the arrival time (t_A) versus DP for the $[M + 3Li]^{3+}$ ions generated from the linear and cyclic samples, and, as observed from Figure 4B, the $[c\text{-PLLA}_{20} + 3Li]^{3+}$ ions remain nicely separated from their linear counterparts upon IMS-MS before the folding. The discussion on the MS-CID-IMS-MS experiments presented in Figure 5 for the sodiated polymers is also still valid for the lithiated species (Figure S8, supporting information).

Similar to the SY method,[14] we use the standards addition method to determine the degree of contamination and, thus, we must prepare samples with different *apparent* cyclic:linear polymer molar ratios. In this procedure, the cyclic and the linear samples are considered as pure, although we already suspect that the cyclic sample is contaminated by residual linear polymer chains (Figure 5). Each sample is analyzed using ESI-IMS-MS, and we observe the steady growth in the abundance of the linear ions (from C10:0 L to C1:9L) by monitoring the evolution of the ATD (Figure 8).

For each DP and each apparent linear-to-cyclic proportion, the IMS traces are deconvoluted, fitted with one or multiple Gaussian curves, and integrated (Figure 9A). The relative proportion of the linear ions is estimated by the surface ratio of the deconvoluted signals, say $A_{total} = A_{linear} + A_{cyclic}$. The ratio is then plotted against the *apparent* proportion of linear polymer in the polymer mixture to build a calibration curve using a linear regression (Figure 9B). The amount of linear contaminants for a given DP in the initial cyclic polymer can then be obtained as the absolute value of the intercept between the linear curve and the *x*-axis.[14]

This method is applied to each DP ranging from 17 to 25. Below 17, the signal-to-noise ratio is too weak to permit effective signal deconvolution, whereas above DP 25, as the complete folding point of the 3+ ions is reached for both sodium and lithium ions, all the signals are merged (Figure 4). While linear curves are expected, only power relationships, that is, $y = Ax^B$, give acceptable coefficients of determination (R^2) for all the investigated DPs (Figure 10A,B and Table SI1, supporting information). Indeed, for low DPs and when a linear trend is used, the coefficient of determination of the linear

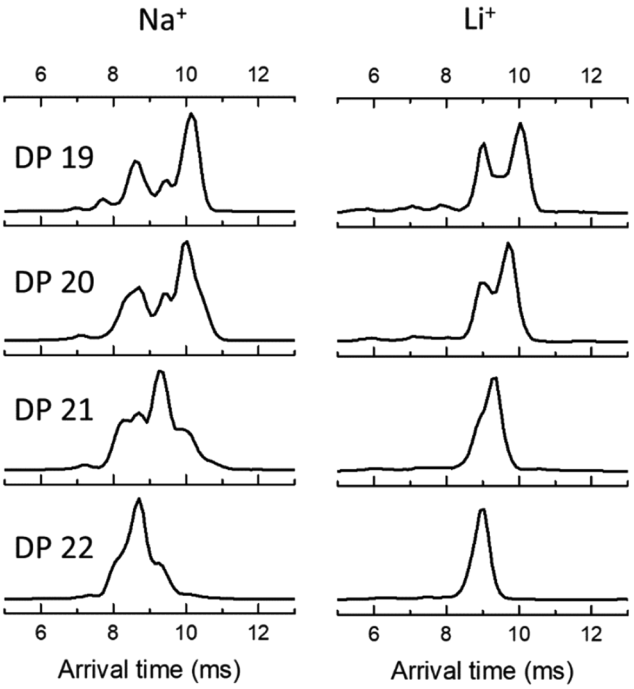

FIGURE 7 Comparison of the ATD of $[l\text{-PLLA}+3Na]^{3+}$ and $[l\text{-PLLA} +3Li]^{3+}$ ions from DP 19 to 22 recorded under soft conditions. No collisional activation is performed before the mobility cell

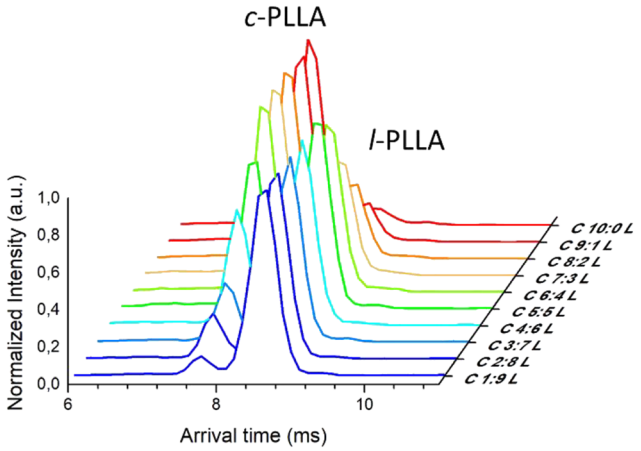

FIGURE 8 Evolution of the ATD for $[PLLA_{24} + 3Li]^{3+}$ ions when increasing the ratio of linear polymer **1** in the cyclic sample [Color figure can be viewed at wileyonlinelibrary.com]

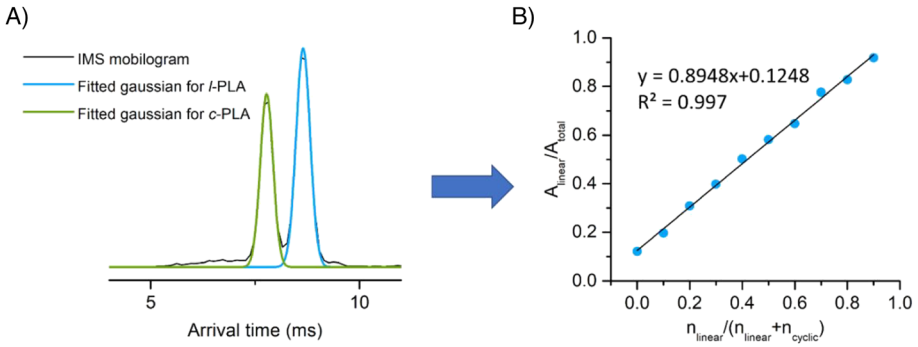

FIGURE 9 A, Deconvolution of the IMS trace with Gaussian fits for DP 24 5:5 mixture and B, correlation between A_{linear}/A_{total} and the relative amount of linear polymer **1** added in the sample for DP 24 [Color figure can be viewed at wileyonlinelibrary.com]

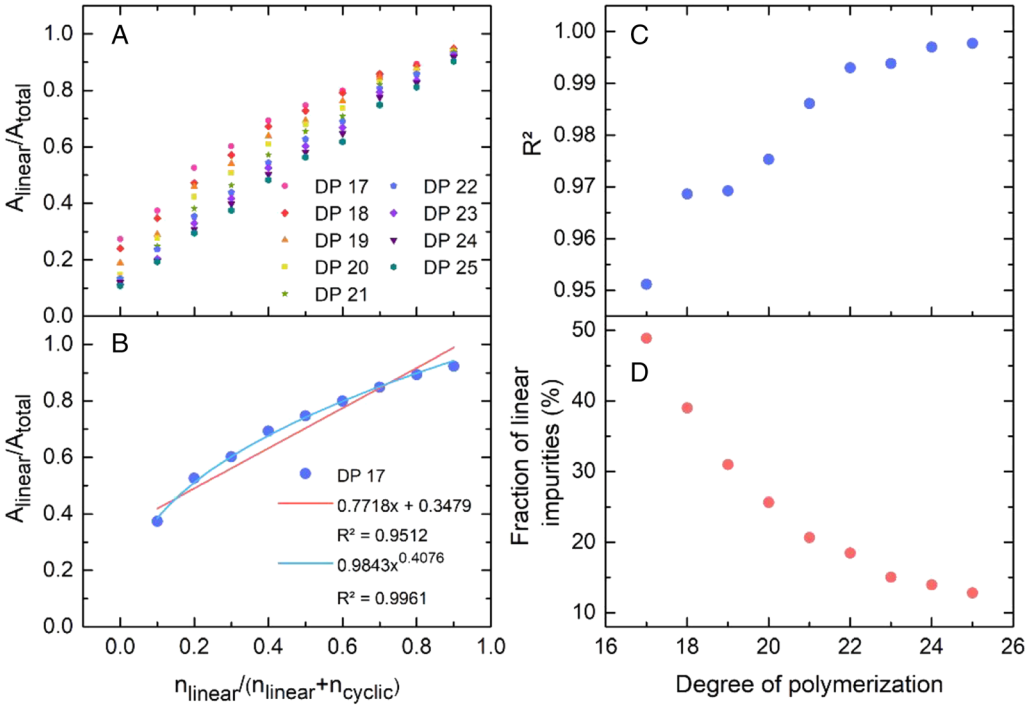

FIGURE 10 A, correlation between A_{linear}/A_{total} and the molar ratio of *l*-PLLA **1** in the sample for DPs ranging from 17 to 25; B, particular case for DP 17 with comparison between the linear and power regressions; C, evolution of the R^2 value for the linear regressions versus DP; and D, evolution of the fraction of linear impurities determined using linear regressions versus DP.[14] [Color figure can be viewed at wileyonlinelibrary.com]

regression is very poor (~0.95; Figure 10B) but it improves as the DP increases and is very close to 1 for DPs 24 and 25 (Figure 10C).

When using the standard addition method (see experimental part) based on a linear calibration, the absolute value of the *x*-axis intercept provides access to the fraction of linear contaminants in the initial cyclic polymer sample.[14] The percentage of linear contaminants is calculated using a linear fitting, even for low DPs presenting a relatively low R^2. As reported in Figure 10D, the contamination by linear by-products is largely overestimated for the lowest DP. For example, by tentatively imposing a linear equation on DP 17 (Figure 10B) with a weak R^2 = 0.9512, we erroneously estimate there to be about 49% of linear polymer in the cyclic sample. The same procedure has been used for all the DPs before the folding (17 to 25) and the linear contamination per DP is reported in Figure 10D and Table SI1 (supporting information). Interestingly, the percentage of linear contaminants decreases when the DP increases, from 49% for DP 17 to 12.8% for DP 25. This decrease is at odds with the Jacobson-Stockmayer theory that predicts more contamination with longer chains.[23] This difference is likely to be associated with different ionization efficiencies between the linear and the cyclic polymer chains. These ionization efficiencies are dependent on the polymer topology (linear vs cyclic), the DP, and the charge state. We suspect that it is less convenient for cyclic polymer chains to accommodate three cations, particularly at low DPs. Globally, the linear contamination is overestimated, especially at low DPs and high charge states. This was already observed in Figure 2 when the ESI

mass spectra of the linear and the cyclic polymers were compared, with the 3+ ions series being more intense for the linear sample. Considering all the previous discussion, the contamination of the sample is best described, for a given charge state, at the highest DP just before the folding point. For the $[M + 3Li]^{3+}$ ions, this corresponds to DP 25 with a corresponding value of around 12.8% of linear contaminants, but this would probably still be an overestimate.

To shed some light on the possible difference of ionization efficiency, we fit the experimental data with theoretical values. As presented in Equation 1, the *y*-axis values in Figures 10A and 10B correspond to the relative abundance of linear ions for a given DP, as measured based on signal integration (A_{linear} and A_{cyclic}, *A* standing for area). In the limits of the dynamic range imposed by the instrument, the number of ions constituting the ion beam is proportional to the number of molecules in the starting sample, with $n_{l\ real}$ and $n_{c\ real}$ representing the real number of moles of the linear and the cyclic polymers in the sample (for a given DP), the proportionality factor being the *ionization efficiency factor* (*IF*) (see Equation 1). Weassume here that no discrimination between cyclic and linear ions is due to the ion transmission and ion detection.

In Equation 2, we define $n_{l\ real}$ as the sum of $n_{l\ th}$, that is, the quantity of the linear isomers introduced in the sample through the standard addition method, and $n_{l\ impurity}$, the quantity of linear impurities present in the cyclic sample. For the cyclic isomer, $n_{c\ real}$ is the quantity of the cyclic isomers really present in the cyclic sample (Equation 3). Finally, we also define K_i as the ratio between the *IF*s of the linear and the cyclic isomers, IF_{linear} and IF_{cyclic}, for a given DP (Equation 4). Equation 1 can thus be modified in Equation 5 that reveals that a linear relationship between the linear ion proportion (*y*-axis in Figure 9B) and the *apparent* proportion of linear polymers in the polymer mixture (*x*-axis) is not achieved.

$$\frac{A_{linear}}{A_{linear} + A_{cyclic}} = \frac{n_{l\ real}.IF_{linear}}{n_{l\ real}.IF_{linear} + n_{c\ real}.IF_{cyclic}} \tag{1}$$

$$n_{l\ real} = n_{l\ th} + n_{l\ impurity} \tag{2}$$

$$n_{c\ real} = n_{c\ th} - n_{l\ impurity} \tag{3}$$

$$K_i = \frac{IF_{linear}}{IF_{cyclic}} \tag{4}$$

$$\begin{aligned}\frac{A_{linear}}{A_{linear} + A_{cyclic}} &= \frac{n_{l\ real}.IF_{linear}}{n_{l\ real}.IF_{linear} + n_{c\ real}.IF_{cyclic}} \\ &= \frac{\left(n_{l\ th} + n_{l\ impurity}\right).IF_{linear}}{\left(n_{l\ th} + n_{l\ impurity}\right)IF_{linear} + \left(n_{c\ th} - n_{l\ impurity}\right).IF_{cyclic}} \\ &= \frac{\left(n_{l\ th} + n_{l\ impurity}\right).K_i}{\left(n_{l\ th} + n_{l\ impurity}\right).K_i + \left(n_{c\ th} - n_{l\ impurity}\right)}\end{aligned} \tag{5}$$

$$\frac{A_{linear}}{A_{linear} + A_{cyclic}} = \frac{n_{l\ real}}{n_{l\ real} + n_{c\ real}} \tag{6}$$

$$\begin{aligned}Y &= \frac{A_{linear}}{A_{linear} + A_{cyclic}} = \frac{n_{l\ real}}{n_{l\ real} + n_{c\ real}} \\ &= \frac{n_{l\ th} + n_{l\ impurity}}{n_{l\ th} + n_{l\ impurity} + n_{c\ th} - n_{l\ impurity}} = \frac{n_{l\ th}}{n_{l\ th} + n_{c\ th}} + \frac{n_{l\ impurity}}{n_{l\ th} + n_{c\ th}} \\ &= \boldsymbol{X} + \boldsymbol{B}\end{aligned} \tag{7}$$

The ideal case would correspond to $IF_{linear} = IF_{cyclic}$, meaning that the relationship in Equation 1 could be simplified in Equation 6. In that case, as exemplified in Equation 7, there is a linear relationship between the linear ion proportion (*y*-axis in Figure 9B) and the *apparent* proportion of linear polymers in the polymer mixture (*x*-axis). In that ideal case, the *x*-intercept ($Y = 0$ in Equation 7) gives the quantity of linear impurities, and the slope of the linear equation is 1. In Figure 10C, we have already shown that as the DP increases, the linear fitting is better, meaning that the difference between the *IF*s of linear and cyclic isomers is less pronounced for higher DPs.

Using Equation 5, it is possible, for each DP, to theoretically reproduce the experimental data, provided that the quantity of linear contamination, that is, $n_{l\ impurity}$ and the IF ratio K_i are known. As discussed previously, the impurity value determined for DP 25 (12.8%) is probably the most reliable although it is probably overestimated. In our theoretical approach, K_i is then used as the variable parameter to optimize the fitting between the experimental and the theoretical data. As presented in Figure 11 for selected DPs and in Figure S9 (supporting information) for the others, we can define K_i values that allow a quasi-perfect reproduction of the experimental data. We here clearly observe that K_i decreases with increasing DP, demonstrating that as the chain lengthens, the IF_{linear} and IF_{cyclic} values get closer to each other. As reported in Figure 11 and in Figure S10 (supporting information), K_i decreases from 2.3 for DP 17 to ~1.0 for DP 25. A ratio of 1, that is, same ionization efficiency factors, is then expected for a higher DP. However, for our IMS-based quantitative method, in that case, the cyclic and linear isomers are no longer separated by ion mobility beyond DP 25.

We must conclude that, whereas ion mobility is powerful in distinguishing linear from cyclic macromolecules, one should be cautious when using it for quantification purposes. In the current case, the main issue encountered is ascribed to the difference in ionization efficiency of polymer chains presenting drastically different topologies, that is, cyclic versus linear structures, which is related to the analytical approach employed in this study that assumes similar *IF*s for the two isomers. At this stage of the discussion, it is reasonable to wonder why, in our work based on the SY method, the quantification between linear and cyclic polymers was achieved. In that work, the quantification was performed on various polymer ions with relatively high DPs considering their low charge state. Indeed, the polymer ions considered were 2+ PLA ions with 19 repeating units. Those polymer ions are globular, meaning that the ionization efficiency difference between the linear and cyclic polymer species is reduced. This is also highlighted in Figure 10D with the overestimation decreasing when going from DP 17 (49%) to DP 25 (12.8%).

However, without employing the standard addition method, that is, by only determining the linear-to-cyclic proportion (ATD

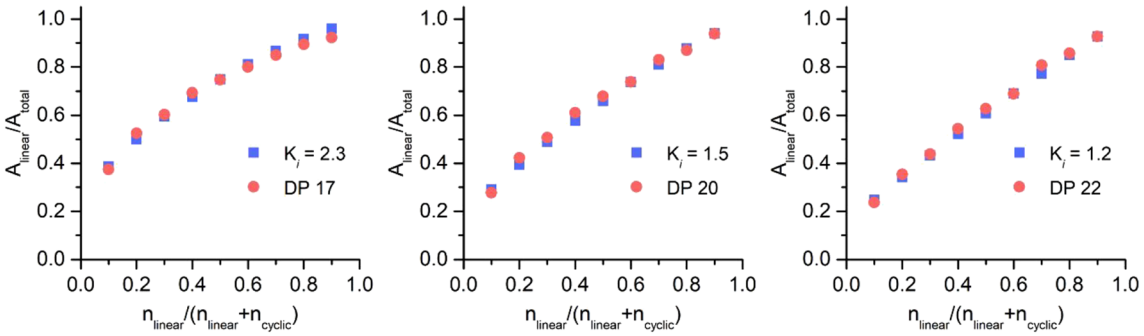

FIGURE 11 Comparison of the experimental data obtained for DPs 17, 20, and 22 and simulated datasets for different K_i values and 12.8% of linear contaminants. Data for DPs 18, 19, 21, 23, and 25 are reported in Figure S9 (supporting information) [Color figure can be viewed at wileyonlinelibrary.com]

integration), the approximate quantity of linear impurity can be estimated based on the highest DP before complete folding (12.8%; Table S1, supporting information).

4 | CONCLUSIONS

A *c*-PLLA was prepared through photodimerization of a linear PLLA end-capped by anthracene moieties. As the SY method to determine the degree of contamination was not useful for this polymer, we wanted to develop a new method using IMS-MS, taking advantage of the fact that IMS can differentiate cyclic polymer ions from their linear analogues because of their more compact 3D conformation before the folding point. It turned out that unrealistically high values of contamination were obtained, which may be explained by an ionization efficiency issue.

Although IMS has proved to be a very powerful tool for polymer characterization, this work underlined some of its limitations in the context of the quantification of isomers. Because of the so-called folding of multiply charged polymer chains, this method could be applied only to a limited range of DPs (before the folding point). In addition, both isomer ions should have the same ionization efficiency to avoid one of them being overestimated. This issue is not related to the use of the IMS but to ionization processes as well as the analytical approach that is used for the relative quantification, which assumes that the two species have the same ionization efficiency. However, the issue could certainly be overcome if the ionization efficiency ratio K_i is known. As of now, the most accurate value of the contamination that can be estimated is that of the highest possible DP before the folding point, but it is probably still overestimated. Finally, even if IMS is a perfect tool for qualitative studies of linear and cyclic isomers, the linear-to-cyclic ratio can be roughly estimated based on the highest DP before complete folding of the ions.

ACKNOWLEDGMENTS

The UMONS MS laboratory acknowledges the Fonds National de la Recherche Scientifique (F.R.S.-F.N.R.S.) for its contribution to the acquisition of the Waters Synapt G2-*Si* mass spectrometer and for continuing support. R.L. thanks F.R.I.A. for its financial support thesis grant. Q.D. and O.C. are F.N.R.S. research fellows. The authors would also like to acknowledge the support of the Research and Innovation Staff Exchange (RISE) BIODEST H2020-MSCA-RISE-2017-778092 project.

ORCID

Romain Liénard https://orcid.org/0000-0002-2696-3046
Quentin Duez https://orcid.org/0000-0002-9067-7917
Pascal Gerbaux https://orcid.org/0000-0001-5114-4352
Julien De Winter https://orcid.org/0000-0003-3429-5911

REFERENCES

1. Altintas O, Yankul B, Hizal G, Tunca U. A_3-type star polymers via click chemistry. *J Polym Sci A Polym Chem*. 2006;4(21):6458-6465. https://doi.org/10.1002/pola.21728
2. Altintas O, Demirel AL, Hizal G, Tunca U. Dendrimer-like Miktoarm star Terpolymers: A_3-(B-C)$_3$ via click reaction strategy. *J Polym Sci A Polym Chem*. 2008;46(17):5916-5928. https://doi.org/10.1002/pola.22908
3. Hoskins JN, Grayson SM. Synthesis and degradation behavior of cyclic poly(ϵ-Caprolactone). *Macromolecules*. 2009;42(17):6406-6413. https://doi.org/10.1021/ma9011076
4. Liénard R, Zaldua N, Josse T, et al. Synthesis and characterization of double crystalline cyclic diblock copolymers of poly(ϵ-caprolactone) and poly(L(D)-lactide) (c (PCL-b-PL(D)LA)). *Macromol Rapid Commun*. 2016;37(20):1676-1681. https://doi.org/10.1002/marc.201600309
5. Zaldua N, Liénard R, Josse T, et al. Influence of chain topology (cyclic versus linear) on the nucleation and isothermal crystallization of poly (l-lactide) and poly(d-lactide). *Macromolecules*. 2018;51(5):1718-1732. https://doi.org/10.1021/acs.macromol.7b02638
6. Laurent BA, Grayson SM. Synthetic approaches for the preparation of cyclic polymers. *Chem Soc Rev*. 2009;38(8):2202-2213. https://doi.org/10.1039/b809916m
7. Hoskins JN, Grayson SM. Cyclic polyesters: Synthetic approaches and potential applications. *Polym Chem*. 2011;2:289-299. https://doi.org/10.1039/c0py00102c
8. Josse T, De Winter J, Gerbaux P, Coulembier O. Cyclic polymers by ring-closure strategies. *Angew Chem Int Ed*. 2016;55(45):13944-13958. https://doi.org/10.1002/anie.201601677
9. Chang YA, Waymouth RM. Recent Progress on the synthesis of cyclic polymers via ring-expansion strategies. *J Polym Sci A Polym Chem*. 2017;55:2892-2902. https://doi.org/10.1002/pola.28635

10. Gao L, Oh J, Tu Y, Chang T, Li CY. Glass transition temperature of cyclic polystyrene and the linear counterpart contamination effect. *Polymer*. 2019;170:198-203. https://doi.org/10.1016/j.polymer.2019.03.018
11. Hadziioannou G, Cotts PM, ten Brinke G, et al. Thermodynamic and hydrodynamic properties of dilute solutions of cyclic and linear polystyrenes. *Macromolecules*. 1987;20(3):493-497. https://doi.org/10.1021/ma00169a006
12. Rique-Lurbet L, Schappacher M, Deffieux A. A new strategy for the synthesis of cyclic polystyrenes: Principle and application. *Macromolecules*. 1994;27(22):6318-6324. https://doi.org/10.1021/ma00100a014
13. Memboeuf A, Jullien L, Lartia R, Brasme B, Gimbert Y. Tandem mass spectrometric analysis of a mixture of isobars using the survival yield technique. *J am Soc Mass Spectrom*. 2011;22(10):1744-1752. https://doi.org/10.1007/s13361-011-0195-8
14. Josse T, De Winter J, Dubois P, Coulembier O, Gerbaux P, Memboeuf A. A tandem mass spectrometry-based method to assess the architectural purity of synthetic polymers: A case of a cyclic polylactide obtained by click chemistry. *Polym Chem*. 2015;6(1):64-69. https://doi.org/10.1039/C4PY01087F
15. Kim K, Lee JW, Chang T, Kim HI. Characterization of polylactides with different stereoregularity using electrospray ionization ion mobility mass spectrometry. *J am Soc Mass Spectrom*. 2014;25(10):1771-1779. https://doi.org/10.1007/s13361-014-0949-1
16. Li X, Guo L, Casiano-Maldonado M, Zhang D, Wesdemiotis C. Top-down multidimensional mass spectrometry methods for synthetic polymer analysis. *Macromolecules*. 2011;44(12):4555-4564. https://doi.org/10.1021/ma200542p
17. Hoskins JN, Trimpin S, Grayson SM. Architectural differentiation of linear and cyclic polymeric isomers by ion mobility spectrometry-mass spectrometry. *Macromolecules*. 2011;44(17):6915-6918. https://doi.org/10.1021/ma2012046
18. Yang J, Wang Y, Rassat A, Zhang Y, Sinaÿ P. Synthesis of novel highly water-soluble 2:1 cyclodextrin/fullerene conjugates involving the secondary rim of β-cyclodextrin. *Tetrahedron*. 2004;60(52):12163-12168. https://doi.org/10.1016/j.tet.2004.10.015
19. Malkoch M, Schleicher K, Drockenmuller E, et al. Structurally diverse dendritic libraries: A highly efficient functionalization approach using click chemistry. *Macromolecules*. 2005;38(9):3663-3678. https://doi.org/10.1021/ma047657f
20. Karthikeyan J, Yoshikai N. Rhodium (III)-catalyzed directed *Peri*-C–H Alkenylation of anthracene derivatives. *Org Lett*. 2014;16(16):4224-4227. https://doi.org/10.1021/ol501926b
21. Josse T, Altintas O, Oehlenschlaeger KK, et al. Ambient temperature catalyst-free light-induced preparation of macrocyclic aliphatic polyesters. *Chem Commun*. 2014;50(16):2024-2026. https://doi.org/10.1039/c3cc49067j
22. Yamamoto T, Yagyu S, Tezuka Y. Light- and heat-triggered reversible linear-cyclic topological conversion of telechelic polymers with anthryl end groups. *J Am Chem Soc*. 2016;138(11):3904-3911. https://doi.org/10.1021/jacs.6b00800
23. Jacobson H, Stockmayer WH. Intramolecular reaction in polycondensations. I. The theory of linear systems. *J Chem Phys*. 1950;18:1600-1606. https://doi.org/10.1063/1.1747547
24. Lonsdale DE, Bell CA, Monteiro MJ. Strategy for rapid and high-purity monocyclic polymers by CuAAC "click" reactions. *Macromolecules*. 2010;43(7):3331-3339. https://doi.org/10.1021/ma902597p
25. De Winter J, Lemaur V, Ballivian R, et al. Size dependence of the folding of multiply charged sodium cationized polylactides revealed by ion mobility mass spectrometry and molecular modelling. *Chem A Eur J*. 2011;17(35):9738-9745. https://doi.org/10.1002/chem.201100383
26. Duez Q, Josse T, Lemaur V, et al. Correlation between the shape of the ion mobility signals and the stepwise folding process of polylactide ions: Stepwise folding process of polylactide ions. *J Mass Spectrom*. 2017;52(3):133-138. https://doi.org/10.1002/jms.3915
27. Larriba C, de la Mora JF, Clemmer DE. Electrospray ionization mechanisms for large polyethylene glycol chains studied through tandem ion mobility spectrometry. *J Am Soc Mass Spectrom*. 2014;25(8):1332-1345. https://doi.org/10.1007/s13361-014-0885-0
28. Larriba C. Fernandez de la Mora J. The gas phase structure of Coulombically stretched polyethylene glycol ions. *J Phys Chem B*. 2012;116(1):593-598. https://doi.org/10.1021/jp2092972
29. Breton GW, Vang X. Photodimerization of anthracene: A [4πs+ 4πs] photochemical cycloaddition. *J Chem Ed*. 1998;75(1):81-82.
30. Galanti A, Santoro J, Mannancherry R, et al. A new class of rigid multi (azobenzene) switches featuring electronic decoupling: Unravelling the isomerization in individual photochromes. *J Am Chem Soc*. 2019;141(23):9273-9283. https://doi.org/10.1021/jacs.9b02544

SUPPORTING INFORMATION

Additional supporting information may be found online in the Supporting Information section at the end of the article.

How to cite this article: Liénard R, Duez Q, Grayson SM, Gerbaux P, Coulembier O, De Winter J. Limitations of ion mobility spectrometry-mass spectrometry for the relative quantification of architectural isomeric polymers: A case study. *Rapid Commun Mass Spectrom*. 2020;e8660. https://doi.org/10.1002/rcm.8660